Chinese Journal of Polymer Science Vol. 35, No. 12, (2017), 1524–1539

Chinese Journal of Polymer Science
© Chinese Chemical Society
Institute of Chemistry, CAS
Springer-Verlag GmbH Germany 2017

Molecular Dynamics and Phase Behavior of Polystyrene/Poly(vinyl methyl ether) Blend in the Presence of Nanosilica*

Qi Chen, Min Zuo**, Yi-hu Song and Qiang Zheng
Ministry of Education Key Laboratory of Macromolecular Synthesis and Functionalization, Department of Polymer Science and Engineering, Zhejiang University, Hangzhou 310027, China

Abstract The variation of phase morphology, critical temperature of demixing, and molecular dynamics for polystyrene/poly(vinyl methyl ether) (PS/PVME) blends induced by hydrophilic nanosilica (A200) or hydrophobic nanosilica (R974) was investigated. With the phase separation of blend matrix, A200 migrated into PVME-rich phase due to strong interaction between A200 and PVME, while R974 moved into PS-rich phase. The thermodynamic miscibility and concentration fluctuation during phase separation of blend matrix were remarkably retarded by A200 nanoparticles due to the surface adsorption of PVME on A200, verified by the correlation length ξ near the critical region from rheological measurement and the weakened increment of reversing heat capacity (ΔC_p) during glass transition *via* modulated differential scanning calorimetry (MDSC). The restricted chain diffusion induced by nanosilica still occurred despite no influence of A200 and R974 on the segmental dynamics of homogenous blend matrix. The interactions between nanosilica and polymer components could restrict the terminal relaxation of blend matrix and further manipulate their phase behavior.

Keywords Phase separation; Nanoparticles; Rheology; Molecular dynamics

Electronic Supplementary Material Supplementary material is available in the online version of this article at http://dx.doi.org/10.1007/s10118-017-1980-z.

INTRODUCTION

The incorporation of nanoparticles into a polymer blend matrix can manipulate the phase behavior and morphology evolution of blend matrix and further provide an effective pathway to attain novel nanocomposites with the unique mechanical[1], electronic[2], magnetic[3] or optical properties[4]. Both the kinetics and thermodynamics of blend matrix could be altered by the nanoparticles, specifically, by the interactions between the nanoparticles and matrix components[5–7]. In terms of thermodynamics, both enthalpy and entropy of blending could be altered by the nanoparticles, depending on their topological structure and interaction with polymer[8]. Lipatov[9] reported that the addition of nanoparticles to polymer blend might change the interaction parameter between the components due to their redistribution caused by the preferential adsorption of polymer chains. Ginzburg[10] proposed a simplified thermodynamic theory for polymer blends filled with spherical nanoparticles, where the thermodynamic interaction parameters within polymer components are altered by the nanoparticles, and the interaction between nanoparticles and polymer is counted into the free energy of mixing. For the aspects of kinetics, lots of studies reported the dynamic heterogeneity of polymer induced by

* This work was financially supported by the National Natural Science Foundation of China (No. 51273173), the Fundamental Research Funds for the Central Universities (No. 2017QNA4038) and Zhejiang Natural Science Foundation (No. LY16E030001).
** Corresponding author: Min Zuo (左敏), E-mail: kezuomin@zju.edu.cn
Received March 20, 2017; Revised April 30, 2017; Accepted May 17, 2017
doi: 10.1007/s10118-017-1980-z

nanoparticles, such as the altered dielectric loss peaks and reversing heat capacity of α-relaxation, which were attributed to the strong interactions between polymer chains and nanoparticles[11−13]. It was found that the effects induced by nanoparticles, such as the limited segmental dynamics[14], steric hindrance effect[15] or stabilized phase structure[16] could contribute to the restrained kinetics of phase separation. However, the effect of molecular dynamics on the phase behavior of ternary nanoparticle/polymer blend is far from understood, since most of the studies are concerned only with the segmental dynamics and thermodynamics influenced by nanoparticles, which neglect the terminal flow of polymer chains affected by nanoparticles.

Phase separation of binary polymer blend can occur by two different mechanisms, depending on its thermodynamic state[17]: (i) nucleation and growth (NG)[18] in metastable state, and (ii) spinodal decomposition (SD)[19] in unstable state. Spinodal phase separation has been widely studied owing to the unique bi-continuous microscopic phase structure[20]. The kinetics of spinodal decomposition (SD) can be divided into three stages[21]. In the early stage, the concentration fluctuation initiated by random noise drives the pronounced nonlinear diffusion with a specific wavelength which can be described by Cahn-Hilliard linearized theory[22]. Then, both the wavelength and amplitude of concentration fluctuation increase with time in the intermediate stage. In the later stage of spinodal phase separation, the amplitude of concentration fluctuation approaches its equilibrium values with the formation of sharp interface, while the wavelength of concentration fluctuation keeps increasing with self-similar coarsening of domains driven by hydrodynamic flow[23]. Hence, the diffusion and terminal flow of polymer chains play a key role in all the stages of phase separation, but few studies have quantified the terminal relaxation behavior induced by nanoparticles and its contribution to the phase behaviors. The sufficient understanding upon the effect of nanoparticles on molecular dynamics of blend matrix may facilitate the manipulation of phase structure and thus optimize the ultimate performance of polymeric nanocomposites.

Molecular dynamics of polymer/nanoparticle nanocomposites are widely studied by broadband dielectric spectrum (BDS)[24, 25] and dynamic rheology[26, 27]. BDS is a sensitive method to investigate the structure transition and molecular movements of polymer and further distinguish the influence of nanoparticles on the segmental dynamics of polymers in the nanocomposites. Rheology is another effective method to investigate the molecular dynamics of polymer materials, where the relaxation behavior of macromolecular chains manifests itself in viscoelastic response at various frequency (ω) regions. Short-range relaxation such as segmental dynamics can be investigated in high ωs, while long-range relaxation behaviors such as the whole chain diffusion can be studied in the so called terminal regions, which shows a characterized frequency dependence of storage modulus (G') and loss modulus (G'') as $G' \sim \omega^2$ and $G'' \sim \omega^1$ for linear monodisperse or narrower disperse macromolecules. The incorporation of nanoparticles may lead to the breakdown of frequency dependence in terminal regions, owing to the retarded chain diffusion or the formation of rigid nanoparticles network[28].

In this study, thermally induced phase separation in a dynamically asymmetric blend of polystyrene/poly(vinyl methyl ether) (PS/PVME) with nanosilica (SiO_2) was probed systematically using melt rheology, optical microscopy and dielectric spectroscopy in the temperature region near glass transition or above demixing temperature. It has been found that the systems with intrinsic dynamic asymmetry, such as polymer solutions of PS and diethl malonate[29] or PS/PVME blend with near-critical composition[30], often present the so-called viscoelastic phase separation (VPS), where the initial concentration fluctuations could be suppressed by elastic stress generated from the emerged rigid domains, leading to the long-time retention of network structure even with minor blend composition[31]. The blend composition of PS/PVME (50/50, *W*/*W*) and annealing temperature of 120 °C were chosen to ensure the thermodynamic dominant spinodal phase separation in the system[32−34]. To compare the effect of nanoparticles with different surface properties on the dispersion and phase behavior of blend matrix, hydrophilic and hydrophobic SiO_2 nanoparticles were both incorporated into PS/PVME (50/50) blend. The effect of hydrophilic and hydrophobic SiO_2 nanoparticles on the segmental dynamics was investigated by dielectric spectra. The morphological evolution during phase separation was assessed using phase contrast microscopy (PCM), and the dispersion state of SiO_2 in the phase-separated blend matrix was observed by transmission electron microscopy (TEM). The evolution of viscoelastic properties was

studied to evaluate the influence of nanoparticles on the onset of phase separation and the flow relaxation of chains for blend matrix.

EXPERIMENTAL

Materials

Polystyrene (PS) and poly(vinyl methyl ether) (PVME) with $M_w^{PS} = 2.8 \times 10^5$ g/mol, $M_w^{PVME} = 8.6 \times 10^4$ g/mol and polydispersity of 2.0 and 1.8 were purchased from Sigma-Aldrich Co. Ltd. Commercial hydrophilic fumed silica Aerosil A200 with specific surface area of (200 ± 25) m^2/g and hydrophobic fumed silica Aerosil R974 with specific surface area of (170 ± 20) m^2/g were obtained from Degussa Corp. Both of their average primary particle sizes are 12 nm and the surface silanol densities of A200 and R974 are 2.5 and 0.39 nm^{-2}, respectively[35].

Sample Preparation

PVME samples packaged in 50 wt% aqueous solution were dried for more than 24 h in vacuum oven at 70 °C. Nanosilica were also dried for 24 h at 120 °C in a vacuum oven before use to remove any moisture or water and then the nanosilica was dispersed in toluene to form the suspension without aggregation through 30 min ultrasonication. A 10 wt% polymer solution of PS/PVME was prepared by continuous mechanical mixing and then the solution was cast on the surface of glass plates. The samples were first kept in a desiccator at 25 °C for 3 days to get rid of most of the solvent and further dried at 40, 50 and 60 °C, respectively in a vacuum oven for 6 days to remove the residual solvent. These films were compression molded into discs with the dimensions of 25 mm in diameter and 1.2 mm in thickness at 10 MPa and 55 °C for rheological measurements. Films with the thickness of 0.1 mm for dielectric spectroscopy and differential scanning calorimetry (DSC) were prepared by quantitative solution casting in the customized glassware and removing the solvent as mentioned above. Samples for phase contrast microscopy (PCM) observation were prepared in the same way as above with the mixture solution weight fraction of 5 wt%. In the context below, we denote PS/PVME blends by *A*/*B* and PS/PVME/silica nanocomposites by *A*/*B*/*x*, where *A* and *B* are the weight fraction of PS and PVME in the blends, respectively, and *x* is the weight content of nanosilica in the total polymer blends.

Characterizations

Dielectric spectra of samples were measured by Novocontrol alpha broadband dielectric analyzer (GmbH Concept 40, Novocontrol Technology, Germany) to study the segmental dynamics of nanocomposites. Frequency sweeps were conducted from 1 Hz to 10^7 Hz at constant temperatures in nitrogen atmosphere. The variation of reversing heat capacity of nanocomposites during glass transition was detected by modulated differential scanning calorimetry (MDSC, Q100, TA instruments, USA) with N_2 purge in the temperature range from −50 °C to 80 °C at a heating rate of 1 K/min, a modulation period of 120 s and a modulation temperature amplitude of 1 °C.

Linear viscoelasticity of polymer blends and nanocomposites was examined by an Advanced Rheology Expanded System (ARES-G2, TA Instruments, USA) with 25 mm parallel-plate geometry. The samples were annealed at 70 °C before experiments to relieve the internal stress. Dynamic temperature sweep experiments were carried out to attain the phase separation temperature of systems, with a heating rate of 0.5 K/min and a fixed frequency of 0.2 rad/s. Dynamic frequency sweep experiments were employed at diverse temperatures to attain the temperature dependent viscoelasticity. Dynamic time sweep experiments were conducted at 120 °C and 1 rad/s. The strain for all the experiments was kept at 1% to ensure the linear viscoelastic behavior.

The morphological evolution of PS/PVME blends, PS/PVME/A200 and PS/PVME/R974 nanocomposites was detected by phase contrast microscopy (PCM, B1-PH, Motic, China) in combination with a digital camera (Nikon-4500, Nikon, Japan). The samples were isothermally annealed at 120 °C. All the morphological images were recorded in real time online.

Transmission electron microscopy (TEM, JEM 1200EX, Japan) was used to observe the dispersion of

nanoparticles in the blend matrix. Samples subjected to annealing for different time at 120 °C were quenched under liquid nitrogen to attain their morphology. TEM specimens with the thickness of approximately 500 Å were obtained by cryo-microtoming at −100 °C to ensure no alteration of the morphology during cutting.

RESULTS AND DISCUSSION

Segmental Dynamics and Miscibility Induced by Nanosilica

Spinodal decomposition of polymer blend proceeds with the evolution of concentration fluctuation, which is associated with the segmental relaxation and chain diffusion as proposed by de Gennes[36] and Pincus[37]. To further study the molecular dynamics on the phase behaviors of polymer blend in presence of nanoslica, the influence of nanosilica on the segmental dynamics of PS/PVME blends was investigated by broadband dielectirc spectroscopy (BDS). It is widely accepted that dielectric loss peaks measured for PS/PVME blend should be only attibuted to the segmental dynamics of PVME since the dipole moment of PS is much smaller than that of PVME, resulting in negligible contribution of PS to the dielectirc loss of PS/PVME blend[38]. Figure 1 shows the frequency dependence of dielectric loss (ε'') for (a) unfilled, filled PS/PVME (50/50) systems and (b) unfilled, filled PVME systems at different temperatures where the segmental dynamics is active within the investigated frequency regions. The broadening of relaxation spectra in Fig. 1(b) compared with those in Fig. 1(a) can be attributed to the dynamic heterogeneity triggered by the dispersed concentration due to the incorporation of hetero-contacts such as blending with polymer or filling with nanoparticles[39]. However, the presence of nanoparticles hardly causes the variation of frequency for dielectric loss peaks corresponding to segmental dynamics (α relaxation) of PVME, indicating that the nanoparticles can hardly retard the segmental dynamics of PVME in both homopolymer and homogeneous blend matrix. The unaltered glass transition (T_g) or segmental relaxation time (τ_{seg}) with the incorporation of nanoparticles were also found in other nanocomposties, such as poly(vinyl acetate)/nanoslica[40], poly(ether imide)/fumed silica and poly(methyl methacrylate)/fumed silica nanosomposites[41]. However, it was also reported that the restriction of segmental mobility induced by nanoparticles was treated as the origin of retarded kinetics of phase separation[14, 33, 42]. Herein, the unaltered segmental dynamics may indicate the indirect correlation between segmental dynamics and phase separation. Figure 2 shows the variation of reversing heat capacity (ΔC_p) during glass transition for unfilled and filled PS/PVME 50/50 systems. It can also be found that the glass transition temperature (T_g) values of PS/PVME/nanosilica nanocomposites blend hardly change with the incorporation of nanosilica. However, the ΔC_p values decrease in nanosilica filled blends, especially in A200 filled blends. It was proposed by Donth's approximation[43] that the volume of cooperative rearranging region (V_a) could be evaluated by the equation

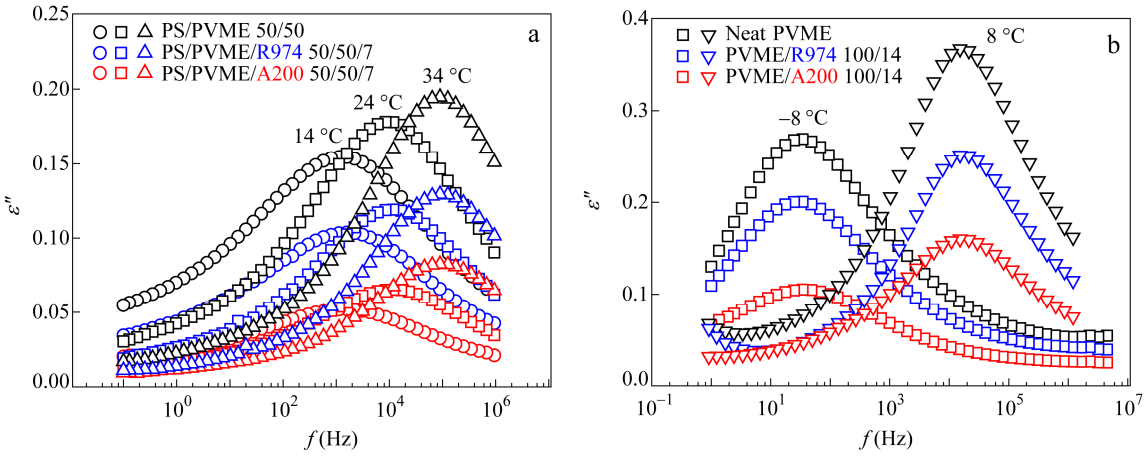


Fig. 1 Normalized dielectric loss peaks of (a) unfilled and filled PS/PVME (50/50) systems at 14, 24 and 34 °C and (b) unfilled and filled PVME systems at −8 and 8 °C

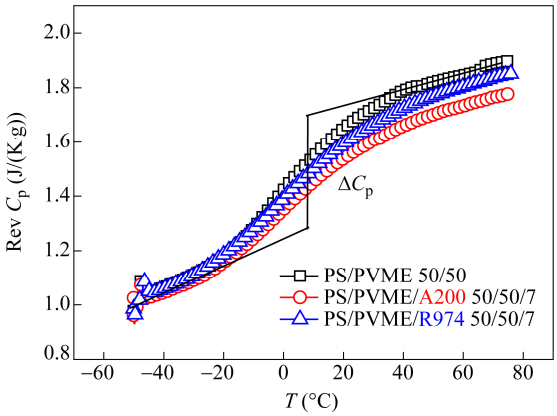


Fig. 2 Normalized specific reversing heat capacity of unfilled and filled PS/PVME 50/50 blends through the glass transition (The solid lines indicate the method to determine ΔC_p.)

$$V_a = \frac{kT_g^2}{\Delta C_p \rho (\delta T)^2} \tag{1}$$

where ρ is the density of bulk material, δT is the half-width of T_g. Thus, the decrease of ΔC_p induced by nanosilica results in the increment of V_a, indicating that the incorporation of nanosilica may enhance the miscibility of PS/PVME 50/50 blend matrix[42].

To examine the contribution of nanoparticles on the thermodynamic miscibility of blend matrix, isochronal dynamic temperature sweep tests were carried out based on the sensitive response of viscoelastic change for polymer blends in the homogeneous region and phase-separated region or pre-transition region, especially at low angular frequencies (ωs)[44, 45]. The effect of nanoparticles on the thermodynamics of phase separation for the blend matrix can be investigated based on the theory of Ajii and Choplin[46], which was introduced into the study of phase separation near the critical point for binary polymer blends as the extension of Fridrickson and Larson's mean field theory describing the order-disorder transition of block copolymers[47]. Recently, the theory has been widely employed in ternary particle-filled blends to investigate the thermodynamics of phase separation for blend matrix. The ratio of elastic modulus and loss modulus at a small strain and low ωs for binary blend near critical point can be calculated as

$$\frac{G'(\omega)}{[G''(\omega)]^2} = \frac{30\pi}{k_B T}\left\{\frac{a_1^2}{36\phi} + \frac{a_2^2}{36(1-\phi)}\right\}^{3/2} (\chi_s - \chi)^{-3/2} \tag{2}$$

where χ is the interaction parameter at temperature T, χ_s denotes the interaction parameter at spinodal temperature, k_B is the Boltzmann coefficient, a_i is the segment length for polymer i. Furthermore, the correlation length ξ of polymer blend obtained by random phase approximation (RPA) is

$$\xi = \frac{a'}{6}[\phi(1-\phi)(\chi_s - \chi)]^{-1/2} \tag{3}$$

where a' is the characteristic length determined by individual segment length as

$$\frac{a'^2}{\phi(1-\phi)} = \frac{a_1^2}{\phi} + \frac{a_2^2}{1-\phi} \tag{4}$$

Then one can obtain the correlation length ξ near the critical region from rheological experiment as

$$\xi = \left[\frac{k_B T G'}{30\pi G''^2}\right]^{1/3} \tag{5}$$

The correlation length ξ, can be expressed as[46, 47]

$$\xi(T, \varphi) = \xi_0(\varphi)\varepsilon^{-n} \tag{6}$$

where $\varepsilon = [(T - T_s)/T_s]$, T_s is the spinodal temperature and $n = 1/2$. Then one can estimate the spinodal decomposition temperature by extrapolating the reciprocal square of correlation length ξ^{-2} to $1/T$ axis and attaining the straight line intercept at $\xi^{-2} = 0$.

Figure 3(a) shows the temperature dependence of correlation length for unfilled and filled PS/PVME (50/50) blends. The temperature dependence of G' for unfilled and filled systems is shown in Fig. S1 (in supporting information, SI) and their correlation length values calculated from Eq. (5) are directly given here. The correlation length ξ, as the reflection of length scale of concentration fluctuation, would increase progressively at the onset of phase separation[33, 46]. As shown in Fig. 3(a), the upturns of correlation length for three systems derive from the promoted concentration fluctuation by phase separation and PS/PVME (50/50) blend shows a more pronounced enhancement of correlation length in the vicinity of phase separation compared with two nanocomposites, indicating that the local concentration fluctuation in the vicinity of phase separation for the blend matrix may be restrained by the incorporation of nanoparticle. Hence, the subtle transition of correlation length near phase boundary for nanosilica filled systems can hardly be used to directly distinguish the phase separation temperature. Also, the change of ξ for PS/PVME/R974 (50/50/7) is more obvious than that for PS/PVME/A200 (50/50/7), suggesting that A200 may induce the miscibility at molecular length scales. The temperatures for three systems (T_s) are determined by extrapolating the reciprocal square of correlation length ξ^{-2} near the phase boundary to $1000/T$ axis and their error bar is 2 °C, as depicted in Fig. 3(b). The increments of T_s for PS/PVME/R974 (50/50/7) and PS/PVME/A200 (50/50/7) nanocomposites are 3.5 and 6.4 °C, respectively, indicating that the presence of nanoparticles may retard the concentration fluctuation and enhance the miscibility, especially for A200 filled system.

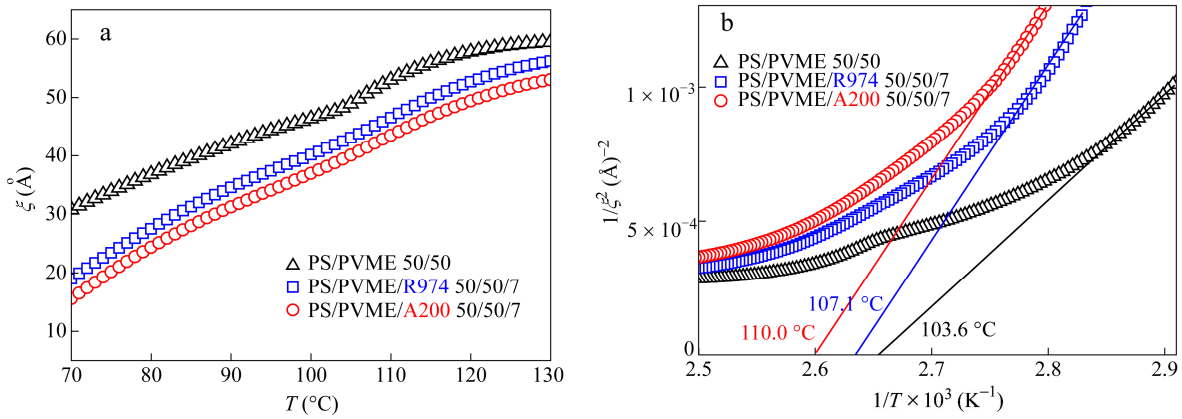


Fig. 3 (a) Temperature dependence of correlation length of concentration fluctuation for PS/PVME 50/50, PS/PVME/A200 50/50/7 and PS/PVME/R974 50/50/7 mixtures in the vicinity of phase separation temperature; (b) Determination of spinodal temperatures of PS/PVME 50/50, PS/PVME/A200 50/50/7 and PS/PVME/R974 50/50/7 mixtures (The solid lines denote method to estimate the spinodal temperatures of samples.)

Some experiments and simulations have also observed the enhanced miscibility in polymer blends filled with nanoparticle[48–53]. For example, Bharati *et al.*[54] suggested that the interaction between silver nanoparticle and polymer matrix might induce the miscibility and slower the phase separation in PS/PVME system by evaluating the evolution of correlation length nearby phase separation temperature. Ginzburg[10] also proposed a thermodynamic model to study the effect of nanoparticles on the miscibility of polymer blend and recalculated the free energy in the ternary system by taking both the particle size and particle-polymer interaction into consideration. The radius of primary particles (12–16 nm) in this study is comparable with the polymer radius of

gyration (10–15 nm)[55], which reduces the number of unfavorable PS-PVME interaction and therefore depresses the enthalpy contribution of free energy, leading to the enhancement of miscibility as suggested by the model. Moreover, it was proposed by Lipatov *et al.*[56] and Nesterov *et al.*[57] that an "interfacial layer" may form on the surface of nanoparticles due to the preferential adsorption of the components of polymer blend on the nanoparticles, in which the polymer conformation and composition differ from the blend matrix. Namely, the interaction within particle-polymer may also contribute to the enhancement of miscibility[58]. Here, the silanol groups on the surface of hydrophilic A200 nanoparticles are much more than those on the surface of hydrophobic R974 particles, resulting in more hydrogen bonds forming between the silanol group on the surface of A200 and the ether bond of PVME[7, 32]. Hence, it can be concluded from Fig. 3 that a higher increment of cooperative rearranging region in A200 filled blend might be attributed to the stronger interactions within A200 filled blends than those in R974 filled blends. Moreover, adsorption of PVME on the surface of A200 induced by the strong interaction may result in the increase of PS composition in the blend matrix, which also contributes to the increment of phase separation temperature depending on its phase diagram.

Morphology Evolution during Phase Separation

The role of nanosilica-polymer interactions in affecting the phase separation of PS/PVME blend matrix may be elucidated by a detailed morphology analysis. Figure 4 shows the PCM micrographs for the morphology evolution of neat PS/PVME (50/50) blend and PS/PVME/silica nanocomposites after being annealed at 120 °C, which is above the spinodal temperature estimated by dynamic rheological temperature sweep, for different periods with the corresponding 2D-FFT pattern insets. The 2D-FFT patterns were obtained by fast Fourier transformation of PCM photos which were described in detail otherwise. All the systems in this study experience the same spinodal decomposition mechanism of phase separation at 120 °C for 60, 300 and 720 min, yielding an interconnected structure at first 60 min and the following coarsening of co-continuous structure[59, 60]. The scattering rings in the 2D-FFT patterns also indicate the evolution of co-continuous structure for these mixtures being annealed at 120 °C[61]. However, our experiments could not be extended far enough to observe the breakup of co-continuous structure driven by interfacial tension for avoiding the oxidation degradation of PVME. Moreover, the wavelength (L) of concentration fluctuation can be estimated by 2D-Fourier transition of PCM micrographs as

$$L = 2\pi / q_{\mathrm{m}} \tag{7}$$

where q_{m} is the wave vector of the fastest growing concentration fluctuation and proportional to the diameter of 2D-FFT ring[18]. It can be found from Fig. 4 that the domain sizes of the A200 filled systems are remarkably smaller than those of the unfilled system and the scattering ring diameters of the A200 filled systems are bigger than those of the unfilled system, indicating that the addition of A200 may suppress the domain coarsening. Furthermore, the increase of the A200 mass fraction weakens the shrinkage of domain size and the boundary between PS and PVME for PS/PVME/A200 (50/50/7) nanocomposites becomes obscure. However, the domain size of PS/PVME/R974 (50/50/4) nanocomposite is similar with that of PS/PVME/A200 (50/50/2) blend, suggesting that the hindering effect of R974 on the phase separation of blend matrix is much weaker than the effect of A200.

It has been mentioned that growth of domain size (d) at later stage of spinodal phase separation relies on self-similarity coarsening with time (t), which can be characterized by $d \propto t^a$[34, 48]. Figure 5 shows the time evolution of domain sizes for unfilled and filled PS/PVME mixtures, where d values were obtained by Eq. (7). All mixtures follow a power law dependent growth of the d values and the exponents a remarkably reduce for the filled blends with the increase of nanosilica loadings, indicating the restrained coarsening of domains induced by nanosilica at the later stage of spinodal phase separation, especially for A200 filled blends. Figure 6 shows the time evolution of normalized storage modulus for unfilled and filled PS/PVME (50/50) systems at 120 °C and 1 rad/s. The initial drastic increase in the normalized G'/G'_{max} occurs in PS/PVME/A200 (50/50/4) and PS/PVME/R974 (50/50/4) nanocomposites and should be associated with the intense concentration

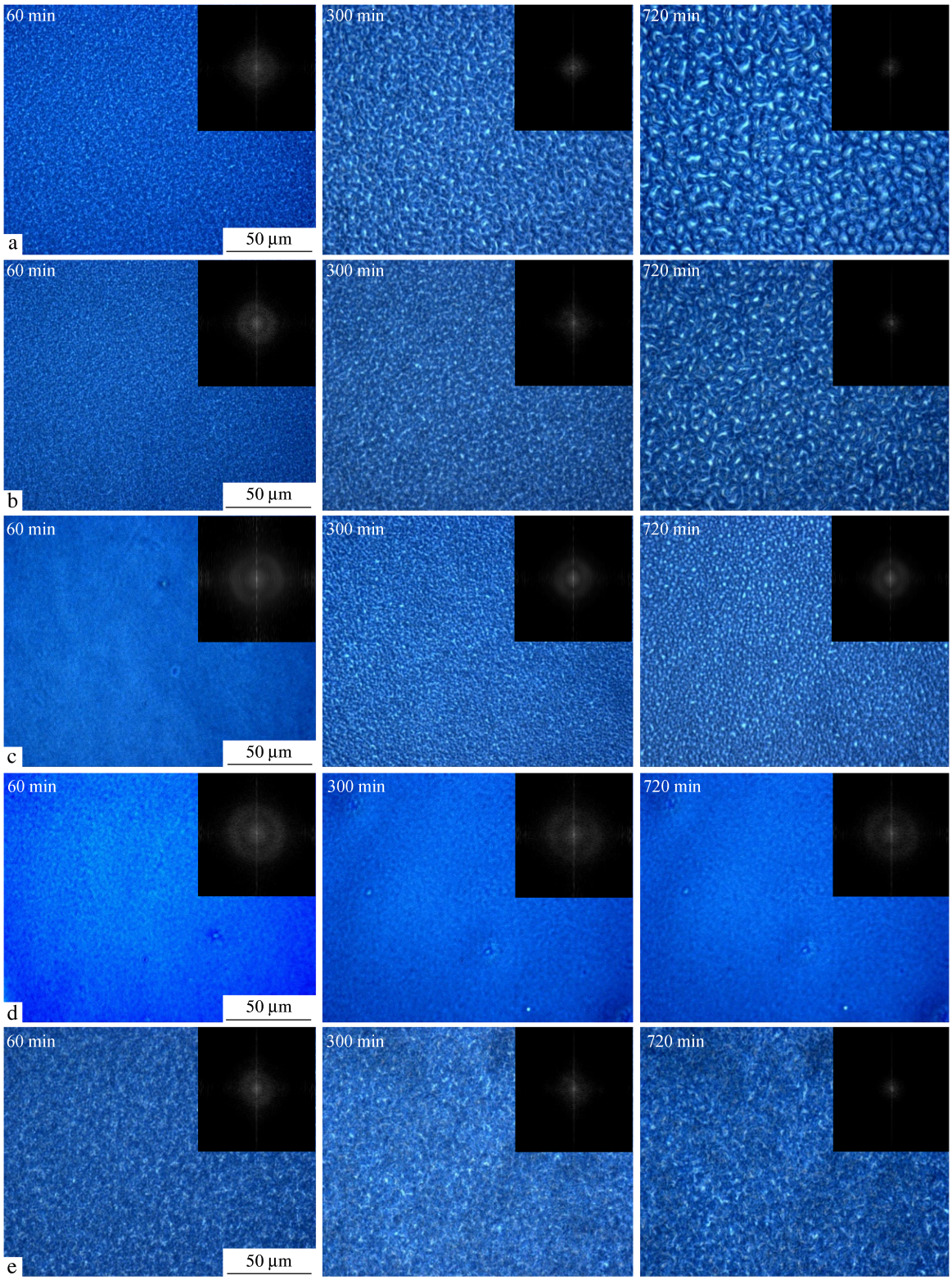


Fig. 4 PCM images of morphology evolution for (a) PS/PVME 50/50, (b) PS/PVME/A200 50/50/2, (c) PS/PVME/A200 50/50/4, (d) PS/PVME/A200 50/50/7 and (e) PS/PVME/R974 50/50/4 systems during phase separation at 120 °C (The scale bar denotes 50 μm. The insets are corresponding 2D-FFT patterns.)

fluctuation and the formation of interface at the early stage of phase separation, while such initial increase in PS/PVME (50/50) blend is too fast to be observed in our study owing to high annealing temperature. The subsequent rapid decrease in G'/G'_{max} is relevant to the coarsening of domain after the saturation of concentration fluctuation. With the incorporation of nanosilica, the decline trend of G'/G'_{max} becomes slower, suggesting a slower phase-separating process, especially for the A200 filled blend. Here, the slower variation of G'/G'_{max} in A200 and R974 filled blends reflects the restricted molecular mobility caused by the selective adsorption of polymer chains on the surface of nanosilica.

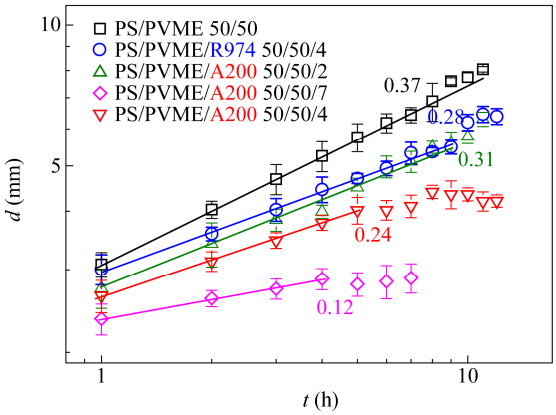


Fig. 5 Time evolution of domain size for unfilled and filled PS/PVME 50/50 systems at 120 °C

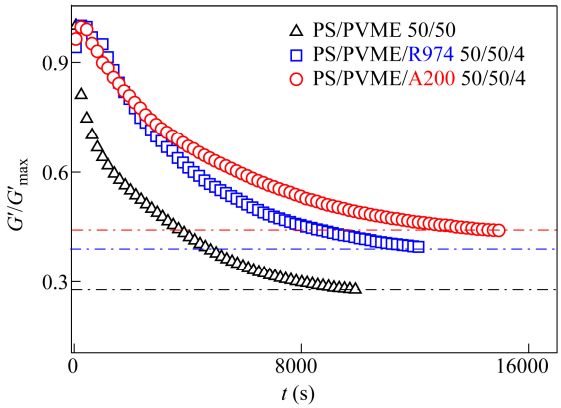


Fig. 6 Time evolution of normalized storage modulus for PS/PVME 50/50, PS/PVME/A200 50/50/4 and PS/PVME/R974 50/50/4 systems at 120 °C

Figure 7 shows the TEM images of PS/PVME/A200 (50/50/4) and PS/PVME/R974 (50/50/4) nanocomposites after being annealed at 120 °C for 1 h. The bright region refers to the PVME-rich phase and the dark region refers to the PS-rich phase in the bright-field TEM images, since PVME is more electronegative (due to its ether bond) and absorbs electrons stronger than PS. It can be found that under the same annealing condition, the domain size in the A200 filled system is remarkably smaller than that in the R974 filled system, which is consistent with the PCM observations. With the phase separation of blend matrix, A200 nanoparticles are dispersed into the PVME-rich phase (bright region), while most of R974 nanoparticles are located in the PS-rich phase (dark region) and small amounts of R974 are dispersed in the PVME-rich phase near the interface. Herein, the interactions between A200 and PVME induced by hydrogen bonds between the silanol group on the surface of A200 and the ether bond of PVME are much stronger than the van der Waals interactions between R974 and PS. Hence, the interaction between the nanoparticles and polymers is likely to increase the thermodynamic affinity, resulting in different selective location of A200 and R974 in the PVME-rich or PS-rich phase[62]. The reduced domain size and the obstacle of coarsening of phase structure for the blend matrix, induced by the interaction within nanoparticle filled polymer blend systems, have been widely observed[48, 49, 63], but the mechanism might be complicated owing to various effects induced by the interaction, such as the constrained segment relaxation[12], chain diffusion[3] or hindered movement of isolated domains[5]. However, the mean segmental dynamics of PVME in PS/PVME blends are hardly changed by A200 and R974 in this work, indicating that the effect of nanosilica on the terminal dynamics, rather than segmental dynamics of polymer chains may play a key role in the coarsening of domains. Therefore, we may speculate that the selective location of A200 in the PVME-rich phase constrain the terminal flow of PVME, and then lead to the more pronounced retardation effect on the phase separation of blend matrix, while the selective location of R974 in the PS-rich phase may have a weaker influence on the terminal flow of PS or PVME chains, which leads to the weaker coarsening retardation effect. On the other hand, the slower kinetics of the filled samples might also be ascribed to the shallower quenching depth because the incorporation of silica could increase the phase separation temperature of blend matrix.

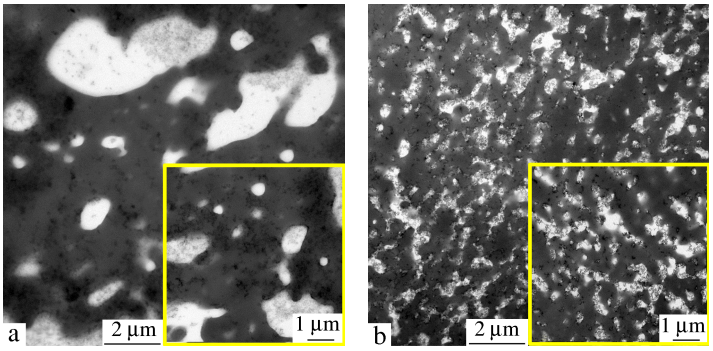


Fig. 7 TEM images of (a) PS/PVME/R974 50/50/4 and (b) PS/PVME/A200 50/50/4 nanocomposites after being annealed at 120 °C for 60 min (The insets are the enlarged patterns.)

Linear Viscoelasticity and Determination of Terminal Relaxation Time

To verify the speculation about the correlation between domain coarsening and terminal flow of polymer chains, linear viscoelasticity of polymer nanocomposites was investigated by dynamic rheological frequency sweep. It has been widely studied that linear viscoelastic response of polymer is sensitive to the slow-down of flow relaxation caused by nanoparticles[64, 65]. Figure 8 shows the master curves of G' and G'' for PVME and PVME/A200 (100/14) nanocomposites at a reference temperature of 70 °C. The temprature region was chosen between 70–90 °C for PVME to obtain the terminal relaxation regions and avoid the possible degradation at 120 °C. The curves obtained from different temperatures can be well surperposed for neat PVME owing to its homogeneous essence. At low ωs, neat PVME exhibits the typical linear viscoelastic behavior chacaterized by scaling laws of $G'(\omega) \sim \omega^2$ and $G''(\omega) \sim \omega^1$ (Fig. 8a). As seen in Fig. 8(b), in the nanocomposites, the ω-dependence of G' and G'' weakens especially at low ωs and there is no G'-G'' crossover, which is the so-called "solid-like" behavior and may be attributed to incomplete relaxation of the filler network occurring simultaneously with the altered relaxation of the polymers contacting nanoparticles[66–68]. Meanwhile, the failure of time-temperature-superposition (TTS) principle in PVME/A200 nanocomposites manifests the thermorheological complexity of PVME/A200 system, which behaves a different temperature dependence of terminal flow relaxation time within system[69, 70]. The thermorheological complexity of filled nanocomposites could be derived from the strong interaction between nanoparticles and polymer matrix, and the aggregation of nanoparticles induced by strong interaction between nanoparticles, especially for A200 filled systems with plenty of hydroxyl groups on the surface of A200 in our study[62]. As shown in Fig. 9, the master curves of G' and G'' for PS and PS/R974 nanocomposites at a reference temperature of 200 °C are also depicted. It should be noted that the scaling law at low ωs for PS does not follow the characterized relationship owing to its strong dependence on the molecular weight distribution of PS. Distinctly, the "solid-like" behavior induced by R974 particles is remarkably weaker than that in PVME/A200 nanocomposites, indicating the slighter alternation of relaxation behavior for PS matrix caused by the weaker interactions within PS/R974 nanocomposites. The temperatures were chosen to approach the terminal flow regions of PS chains. Furthermore, the good agreements of TTS principle in both PS and PS/R974 systems suggest the dynamic homogeneity within PS and PS/R974 nanocomposites. Figure 10 shows the TEM images for PVME/A200 (100/14) and PS/R974 (100/14) nanocomposites to illustrate the dispersion state of nanosilica in PVME or PS matrix. As depicted in Fig. 10, the aggregation of A200 nanoparticles in PVME matrix is more evident than that of R974 in PS matrix. It may derive from the stronger interactions within hydrophilic A200 particles than those among hydrophobic R974 particles, also leading to the more significant thermorheological complexity of PVME/A200 nanocomposites than that of PS/R974 nanocomposites.

The terminal relaxation behavior of polymer chains was altered diversely by A200 and R974, thus, terminal relaxation time of polymer/nanoparticle nanocomposites is quantified to illustrate different effects of A200 and R974 on the terminal relaxation of polymers. Figure 11 shows master curves of $\tan\delta$ for PVME, PS,

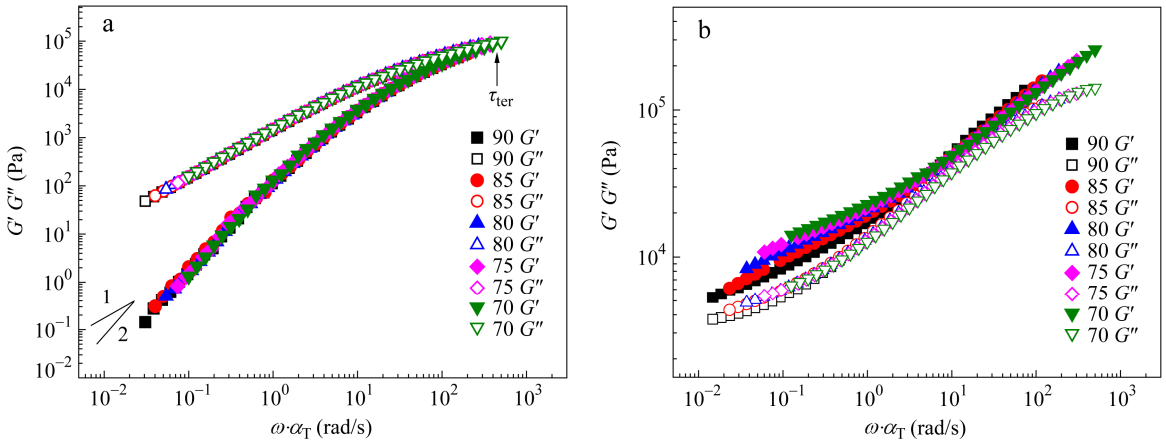


Fig. 8 Master curves of G' and G'' for (a) PVME and (b) PVME/A200 100/14 nanocomposites at the reference temperature of 70 °C

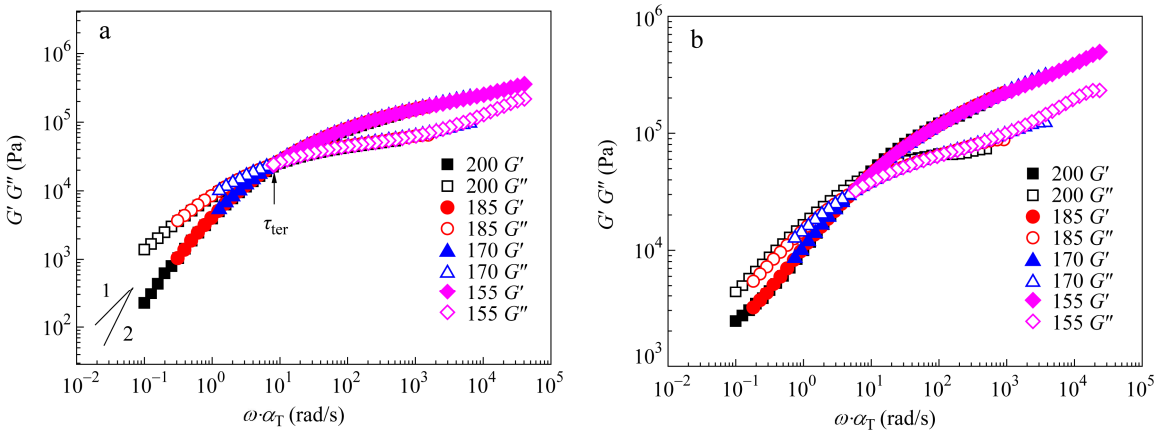


Fig. 9 Master curves of G' and G'' for (a) PS and (b) PS/R974 100/14 nanocomposites at the reference temperature of 200 °C

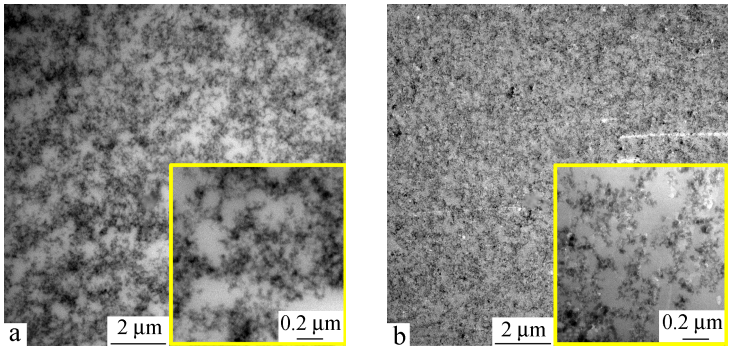


Fig. 10 TEM images of (a) PVME/A200 100/14 and (b) PS/R974 100/14 nanocomposites (The insets are the corresponding enlarged patterns.)

PVME/A200 and PS/R974 systems at the corresponding reference temperatures. The failure of TTS principle in the tanδ curves of PVME/A200 nanocomposites is more remarkable than that of PS/R974 nanocomposites, and the tanδ peaks shift toward high ωs with the increase of A200 loading. To quantify the terminal relaxation time of polymers at 120 °C, terminal relaxation time of neat PVME at 70 °C and PS at 200 °C, τ_{ter}, are determined

firstly as the reciprocal frequency at the G'-G'' crossover. Then, plotting $\tan\delta$ as a function of $\omega\alpha_\phi$ (α_ϕ is the frequency shift parameter) allows creating respective master curve (Figs. 11a and 11b) at the high ω side before the rubbery platform and beyond the Newtonian regime of polymer[71]. Consequently, $\tau_{ter}(\phi)$ of the bulky polymer in the polymer/nanoparticle nanocomposites at 70 and 200 °C can be calculated by $\alpha_\phi \tau_{ter}$, as listed in Table 1. It can be found that A200 significantly restrains the terminal relaxation behavior of PVME, while R974 only shows the relatively weaker restriction on the terminal relaxation of PS chains. Hence, the retarded chain diffusion may occur regardless of how the α-relaxation and T_g change. To further quantify the terminal relaxation time of polymer chains in the nanocomposites at the investigated temperature of 120 °C, the temperature dependence of shift parameters α_T obtained from TTS operation was fitted with the Williams-Landel-Ferry (WLF) or Arrhenius functions. As shown in Fig. 12(a), the shift parameters of PVME and PVME/A200 show a good agreement with Arrhenius function, since the testing temperatures were chosen above 100 °C than T_g of neat PVME. Furthermore, a good agreement of WLF function in PS and PS/R974 systems can be seen in Fig. 12(b) within T_g < testing temperature < (T_g + 100 °C). Consequently, the terminal relaxation time of polymer chains in PVME/A200 and PS/R974 systems at 120 °C can be quantified by the corresponding functions.

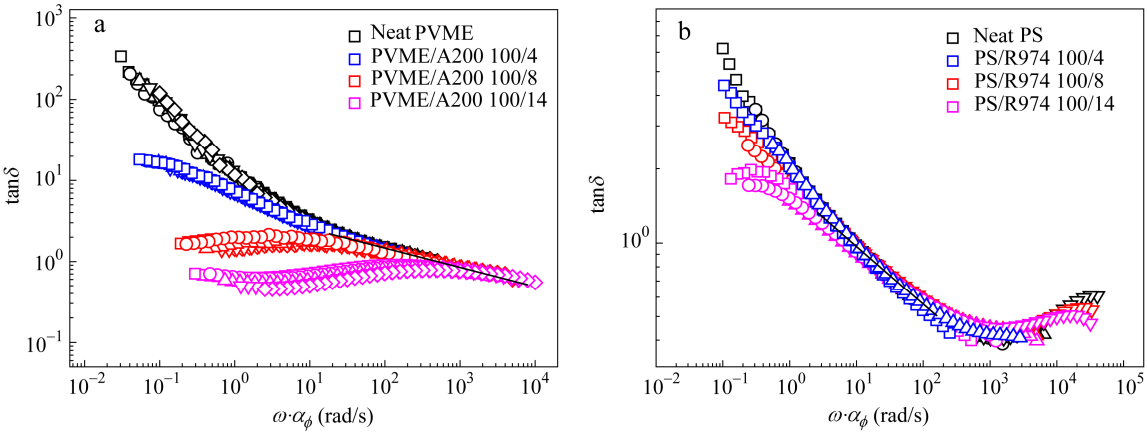


Fig. 11 Master curves of normalized $\tan\delta$ as a function of $\omega\alpha_\phi$ for (a) PVME/A200 nanocomposites at the reference temperature of 70 °C and (b) PS/R974 nanocomposites at the reference temperature of 200 °C

Table 1 Shift parameters and calculated terminal relaxation time of PVME/A200 and PS/R974 nanocomposites at 70 and 200 °C, respectively

Parameter	Sample							
	PVME/A200 at 70 °C				PS/R974 at 200 °C			
	100/0	100/4	100/8	100/14	100/0	100/4	100/8	100/14
α_ϕ	1.0	2.0	10.0	20.0	1.00	1.04	1.08	1.10
$\tau_{ter}(\phi) \times 10^3$ (s)	12.6	25.2	126.0	252.0	775.7	806.7	837.8	853.3

Nanoparticles may slow down the polymer diffusion and the confinement effect may be determined by interparticle spacing and macromolecular size. Figure 13 shows the relative relaxation time, τ_ϕ/τ_{ter}, as a function of nanosilica loading ϕ and the relative diffusion coefficient, $D(\phi)/D_m$, as a function of confinement parameter (ID/2R_g). Here, ID represents the interparticle distance calculated according to ID = $R\{[2/(\pi\phi)]^{1/3}-1\}$ assuming particles with an average diameter R are randomly distributed in the matrix with a radius of gyration of R_g[72]. R_g values of PS and PVME are used as 12.3 and 11.5 nm, respectively, obtained from the literatures[55]. τ_ϕ/τ_{ter} of PVME/A200 systems in Fig. 13(a) increases more strongly than that of PS/R974 systems and $D(\phi)/D_m$ in PVME/A200 systems decreases more remarkably with decreasing ID/2R_g than that in PS/R974 systems, indicating that the diffusion of PVME macromolecules is highly constrained. The strong slowing down may be

attributed to the loss of chain conformations as the molecules squeeze between closely spaced nanoparticles[73], the additional physical constraints due to entanglements and geometric constraints provided by nanoparticles[74], the altered chains packing and friction in the melt[75], and the formation of immobilized layer exhibiting slower or no segmental motion and larger friction[76]. The immobilized chains may partially account for the retarded terminal dynamics[77]. The distinct limitation of A200 on the terminal relaxation of PVME chains results in the restriction of hydrodynamic flow and diffusion of PVME-rich domains during the phase separation of PS/PVME blend, which largely reduces the driving force of coarsening[78, 79]. On the other hand, for R974 filled blends, the hydrodynamic flow and diffusion of domains are slightly altered by the weak interaction within PS/R974 systems.

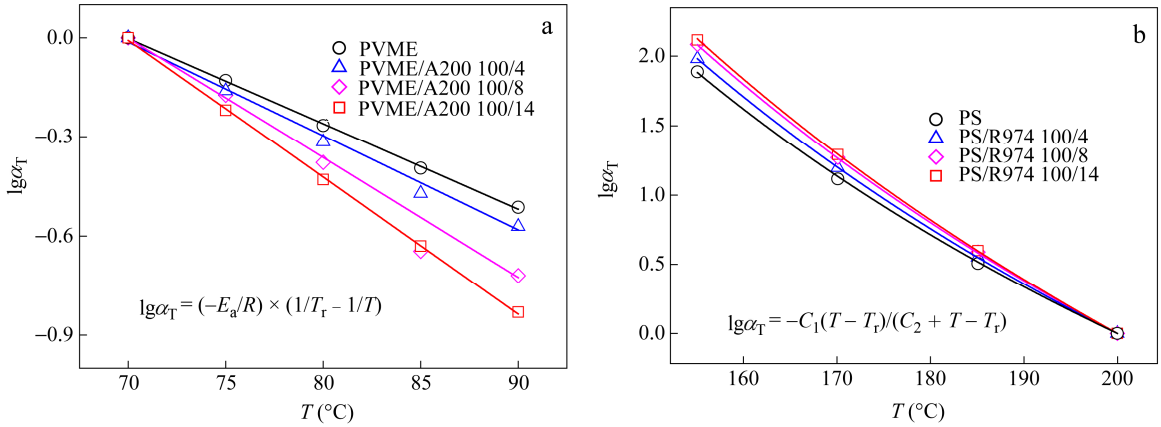


Fig. 12 Temperature dependence of shift factor for (a) PVME/A200 nanocomposites with the reference temperature of 70 °C and (b) PS/R974 nanocomposites with the reference temperature of 200 °C
The solid lines are fitted to Arrhenius function for (a) and WLF function for (b).

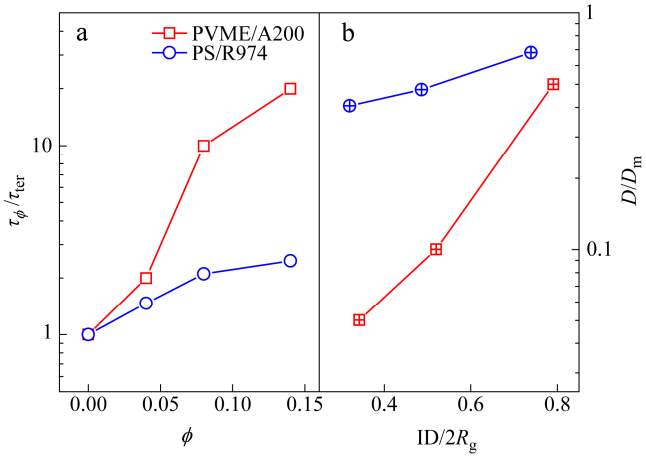


Fig. 13 (a) Relative relaxation time τ_ϕ/τ_{ter} as a function of ϕ and (b) relative diffusion coefficient D/D_m as a function of confinement parameter ID/2R_g for PVME/A200 and PS/R974 systems at 120 °C

Consequently, the phase behavior of PS/PVME 50/50 blends can be manipulated by the interactions within nanocomposites. Besides the reduced thermodynamic driving force induced by shallower quenching depth, it should be the terminal flow dynamics that control the coarsening kinetics of PS/PVME blend, rather than the segmental dynamics. The terminal flow relaxation is highly limited for PS/PVME/A200 nanocomposites owing to the strong hydrogen bonding interactions between PVME and A200, leading to the reduced hydrodynamic

flow and diffusion of PVME-rich domains. On the other hand, the weak van der Waals interactions between R974 and PS show the weak limitation of hydrodynamics flow and diffusion of PS-rich domains. Furthermore, the strong interaction within PS/PVME/A200 system could also lead to larger enthalpic and entropic changes than those of R974 filled blends, resulting in the higher miscibility of blend matrix, which further contributes to the slower kinetics of A200 filled blend than that of R974 filled blends.

CONCLUSIONS

The effect of hydrophilic A200 and hydrophobic R974 on the phase morphology, critical temperature of demixing, local segmental dynamics and molecular mobility of the chains for dynamically asymmetric PS/PVME (50/50) blends was systematically investigated using dynamic shear rheology, morphological observations and dielectric spectroscopy. The remarkable retarded phase separation of PS/PVME/A200 nanocomposites was observed by PCM compared with PS/PVME (50/50) and PS/PVME/R974. With the phase separation of blend matrix, hydrophilic A200 migrated into the PVME-rich phase due to strong interaction between A200 and PVME verified by MDSC results, while hydrophobic R974 moved into the PS-rich phase. The rheologically determined demixing temperatures were enhanced by the incorporation of nanosilica, and the correlation length of concentration fluctuation in the vicinity of separation temperature, determined by Ajii-Choplin' method, was limited by the nanoparticles, especially in the A200 filled nanocomposites, suggesting the enhanced miscibility and suppressed concentration fluctuation induced by the nanoparticles. Although the restriction of A200 on the phase separation of blend matrix was more pronounced than that of R974, A200 or R974 hardly affected the glass transition temperature and mean segmental relaxation time of PVME in PVME based nanocomposites and homogeneous PS/PVME based nanocomposites. Nanosilica might cause a slow-down in the polymer chains diffusion regardless of the effect of nanosilica on the segmental dynamics of blend matrix and the retardation of A200 or R974 on the terminal relaxation of bulky PVME or PS phase was disclosed by creating the ω-dependent curves of $\tan\delta$ superposed in the hydrodynamics-dominated high ω region before approaching the rubbery platform. Here, the constrained terminal relaxation of PVME chains in PVME-rich domains caused by strong interactions between A200 and PVME may suppress the domain coarsening during phase separation, rather than the local segmental dynamics of PVME. The weak interaction between R974 and components of blend matrix and the location of R974 in the PS-rich phase may result in the weakened retardation of phase separation. Hence, the interactions between nanoparticles and components of blend matrix could retard the polymer chain diffusion and further manipulate the morphology evolution and properties of ternary nanocomposites.

REFERENCES

1 Wang, M., Pramoda, K. and Goh, S.H., Polymer, 2005, 46(25): 11510
2 Nair, S.T., Vijayan, P.P., Xavier, P., Bose, S., George, S.C. and Thomas, S., Compos. Sci. Technol., 2015, 116: 9
3 Li, H.H., Zuo, M., Liu, T., Chen, Q., Zhang, J. and Zheng, Q., RSC Adv., 2016, 6(12): 10099
4 Allen, R.C., Kotz, A.L., Carlson, L.W., Nevitt, T.J., Ouderkirk, A.J., Stover, C.A., Weber, M.F. and Majumdar, B., Optical film with co-continuous phases, Google Patents, 2003
5 Huang, C., Gao, J., Yu, W. and Zhou, C., Macromolecules, 2012, 45(20): 8420
6 Gao, J., Huang, C., Wang, N., Yu, W. and Zhou, C., Polymer, 2012, 53(8): 1772
7 Li, H., Li, Q., Li, L. and Yang, Q., J. Macromol. Sci. B, 2014, 53(6): 993
8 Xavier, P., Rao, P. and Bose, S., Phys. Chem. Chem. Phys., 2016, 18(1): 47
9 Lipatov, Y.S., Prog. Polym. Sci., 2002, 27(9): 1721
10 Ginzburg, V.V., Macromolecules, 2005, 38(6): 2362
11 Klonos, P., Panagopoulou, A., Kyritsis, A., Bokobza, L. and Pissis, P., J. Non-Cryst. Solids, 2011, 357(2): 610
12 Lu, H. and Nutt, S., Macromolecules, 2003, 36(11): 4010

13 Yurekli, K., Karim, A., Amis, E.J. and Krishnamoorti, R., Macromolecules, 2003, 36 (19): 7256
14 Xavier, P., Bharati, A., Madras, G. and Bose, S., Phys. Chem. Chem. Phys., 2014, 16(39): 21300
15 Taguet, A., Cassagnau, P. and Lopez-Cuesta, J.M., Prog. Polym. Sci., 2014, 39(8): 1526
16 Li, L., Miesch, C., Sudeep, P., Balazs, A.C., Emrick, T., Russell, T.P. and Hayward, R.C., Nano Lett., 2011, 11(5): 1997
17 Gelb, L.D., Gubbins, K., Radhakrishnan, R. and Sliwinska-Bartkowiak, M., Rep. Prog. Phys., 1999, 62(12): 1573
18 Hashimoto, T., Kumaki, J. and Kawai, H., Macromolecules, 1983, 16(4): 641
19 Snyder, H.L., Meakin, P. and Reich, S., Macromolecules, 1983, 16(5): 757
20 Li, L., Nano Lett., 2011, 11(5): 1997
21 Cahn, J.W., J. Chem. Phys., 1965, 42(1): 93
22 Cahn, J.W. and Hilliard, J.E., J. Chem. Phys., 1958, 28(2): 258
23 Rogers, T., Elder, K. and Desai, R.C., Phys. Rev. B, 1988, 37(16): 9638
24 Kim, D., Srivastava, S., Narayanan, S. and Archer, L.A., Soft Matter, 2012, 8(42): 10813
25 Holt, A.P., Griffin, P.J., Bocharova, V., Agapov, A.L., Imel, A.E., Dadmun, M.D., Sangoro, J.R. and Sokolov, A.P., Macromolecules, 2014, 47(5): 1837
26 Krishnamoorti, R. and Yurekli, K., Curr. Opin. Colloid Interface Sci., 2001, 6(5): 464
27 Galgali, G., Ramesh, C. and Lele, A., Macromolecules, 2001, 34(4): 852
28 Krishnamoorti, R. and Giannelis, E.P., Macromolecules, 1997, 30(14): 4097
29 Tanaka, H., Phys. Rev. Lett., 1993, 71(19): 3158
30 Tanaka, H., Phys. Rev. Lett., 1996, 76(5): 787
31 Tanaka, H., J. Phys. Condens. Matter, 2000, 12(15): R207
32 Ajji, A., Choplin, L. and Prud'Homme, R., J. Polym. Sci., Part B: Polym. Phys., 1988, 26(11): 2279
33 Xavier, P. and Bose, S., J. Phys. Chem. B, 2013, 117(28): 8633
34 Yeganeh, J.K., Goharpey, F., Moghimi, E., Petekidis, G. and Foudazi, R., Soft Matter, 2014**,** 10 (46): 9270
35 Bode, R., Ferch, H. and Fratzscher, H., Tech. Bulletin Fine Particles, 2006, 11(4): 55
36 de Gennes, P.G., J. Chem. Phys., 1980, 72(9): 4756
37 Pincus, P., J. Chem. Phys., 1981, 75(4): 1996
38 Hirose, Y., Urakawa, O. and Adachi, K., Macromolecules, 2003, 36(10): 3699
39 Kumar, S.K., Shenogin, S. and Colby, R.H., Macromolecules, 2007, 40(16): 5759
40 Bogoslovov, R., Roland, C., Ellis, A., Randall, A. and Robertson, C., Macromolecules, 2008, 41(4): 1289
41 Comer, A., Heilman, A. and Kalika, D., Polymer, 2010, 51(22): 5245
42 Xavier, P. and Bose, S., Phys. Chem. Chem. Phys., 2014, 16(20): 9309
43 Donth, E., J. Non-Cryst. Solids, 1982, 53(3): 325
44 Han, C.D., Baek, D.M., Kim, J.K., Ogawa, T., Sakamoto, N. and Hashimoto, T., Macromolecules, 1995, 28(14): 5043
45 Friedrich, C., Schwarzwaelder, C. and Riemann, R.E., Polymer, 1996, 37(12): 2499
46 Ajji, A. and Choplin, L., Macromolecules, 1991, 24(18): 5221
47 Fredrickson, G.H. and Larson, R., J. Chem. Phys., 1987, 86(3): 1553
48 Khademzadeh Yeganeh, J., Goharpey, F., Moghimi, E., Petekidis, G. and Foudazi, R., Phys. Chem. Chem. Phys., 2015, 17 (41), 27446
49 Gao, J., Huang, C., Wang, N., Yu, W. and Zhou, C., Polymer, 2012, 53(8): 1772
50 Xia, T., Huang, Y., Peng, X. and Li, G., Macromol. Chem. Phys., 2010, 211(20): 2240
51 Gharachorlou, A. and Goharpey, F., Macromolecules, 2008, 41(9): 3276
52 Khademzadeh Yeganeh, J., Goharpey, F. and Foudazi, R., Macromolecules, 2010, 43(20): 8670
53 Kar, G.P., Begam, N., Basu, J.K. and Bose, S., Macromolecules, 2014, 47(21): 7525
54 Bharati, A., Xavier, P., Kar, G.P., Madras, G. and Bose, S., J. Phys. Chem. B, 2014, 118(8): 2214
55 Pathak, J.A., Colby, R.H., Floudas, G. and Jérôme, R., Macromolecules, 1999, 32(8): 2553
56 Lipatov, Y.S., Nesterov, A.E., Ignatova, T.D. and Nesterov, D.A., Polymer, 2002, 43(3): 875
57 Nesterov, A.E., Lipatov, Y.S., Horichko, V.V. and Gritsenko, O.T., Polymer, 1992, 33(3): 619
58 Yurekli, K., Karim, A., Amis, E.J. and Krishnamoorti, R., Macromolecules, 2004, 37(2): 507

59 Chung, H.J., Wang, H. and Composto, R.J., Macromolecules, 2006, 39(1): 153
60 Lorén, N., Altskär, A. and Hermansson, A.M., Macromolecules, 2001, 34(23): 8117
61 Snyder, H.L., Meakin, P. and Reich, S., J. Chem. Phys., 1983, 78(6): 3334
62 Xia, T., Huang, Y., Jiang, X., Lv, Y., Yang, Q. and Li, G., Macromolecules, 2013, 46(20): 8323
63 Xavier, P., Sharma, K., Elayaraja, K., Vasu, K.S., Sood, A.K. and Bose, S., RSC Adv., 2014, 4(24): 12376
64 Jancar, J., Douglas, J., Starr, F.W., Kumar, S., Cassagnau, P., Lesser, A., Sternstein, S.S. and Buehler, M., Polymer, 2010, 51(15): 3321
65 Bailly, M., Kontopoulou, M. and El Mabrouk, K., Polymer, 2010, 51(23): 5506
66 Akcora, P., Kumar, S.K., Moll, J., Lewis, S., Schadler, L.S., Li, Y., Benicewicz, B.C., Sandy, A., Narayanan, S. and Ilavsky, J., Macromolecules, 2009, 43(2): 1003
67 Jiao, Y. and Akcora, P., Macromolecules, 2012, 45(8): 3463
68 Cassagnau, P., Polymer, 2008, 49(9): 2183
69 Ngai, K. and Plazek, D., Rubber Chem. Technol., 1995, 68(3): 376
70 Kant, R., Kumar, S.K. and Colby, R.H., Macromolecules, 2003, 36(26): 10087
71 Yu, W., Wang, J. and You, W., Polymer, 2016, 98: 190
72 Wu, S., Polymer, 1985, 26(12): 1855
73 Gam, S., Meth, J.S., Zane, S.G., Chi, C., Wood, B.A., Seitz, M.E., Winey, K.I., Clarke, N. and Composto, R.J., Macromolecules, 2011, 44(9): 3494
74 Schneider, G., Nusser, K., Willner, L., Falus, P. and Richter, D., Macromolecules, 2011, 44(15): 5857
75 Yamamoto, U. and Schweizer, K.S., J. Chem. Phys., 2011, 135(22): 224902
76 ten Brinke, J., Litvinov, V., Wijnhoven, J. and Noordermeer, J., Macromolecules, 2002, 35(27): 10026
77 Harton, S.E., Kumar, S.K., Yang, H., Koga, T., Hicks, K., Lee, H., Mijovic, J., Liu, M., Vallery, R.S. and Gidley, D.W., Macromolecules, 2010, 43(7): 3415
78 Nauman, E.B. and He, D.Q., Chem. Eng. Sci., 2001, 56(6): 1999
79 Xavier, P. and Bose, S., Phys. Chem. Chem. Phys., 2015, 17(22): 14972